

## ADAPTIVE HETERODYNE INTERFEROMETER FOR ULTRASONIC NDE

B. F. Pouet\*, R.K. Ing\*\*, S. Krishnaswamy\*, D. Royer\*\*

\*Center for Quality Engineering and Failure Prevention, Northwestern University, Evanston, Illinois 60208-3020 USA

\*\*Laboratoire Ondes et Acoustique de l'université Paris 7, URA CNRS 1503, ESPCI, 10 rue Vauquelin, 752321 Paris cedex 05, France

### INTRODUCTION

For NDE applications, the remote generation and detection of ultrasound by laser present many advantages over traditional piezo-electric based methods. They provide non-intrusive, point generation and detection with a large frequency bandwidth. For example, it can be used on surfaces of complex geometry and elevated temperature on a production line. Ultrasound generation using absorption of pulse laser energy is well known. Various interferometers for optical detection of ultrasound have been described in the literature [1]. In order for the interferometer to be attractive for NDE applications, the interferometer must also be able to operate, without loss of sensitivity, in an environment where large amplitude low frequency vibrations are generally present. Furthermore, the interferometer must be able to achieve a good sensitivity on rough surfaces. The laser light reflected on a rough surface is characterized by speckles. The random intensity and phase distributions of these speckles require the use of interferometer with large étendue. In addition, the possibility of using an optical fiber in the path of the probe beam without loss in the interferometer sensitivity is highly desirable for applications where access to the specimen is limited. The confocal Fabry-Pérot interferometer [1] has been shown to be well adapted for NDE applications. Unfortunately, since the elimination of the optical side-bands is based on the optical filtering action of the confocal cavity, it is sensitive mostly to high frequencies for a reasonable cavity size, typically above 1MHz for a 1 meter cavity length.

Wave mixing in photorefractive crystals (PRC's) has become an attractive alternative way of realizing wide field of view interferometers. Two-wave mixing in photorefractive crystals is used to create a diffracted beam that acts as a reference beam, matching perfectly the signal beam [2]. The dynamic nature of the recorded grating allows the reference beam to adapt to the change in the signal beam wavefront. The dynamic characteristics mainly depend on the nature of the photorefractive material, the total light intensity in the PRC and other experimental parameters. To date, the still quite long time response of the photorefractive effect for real-life applications, where limited amount of light is available, is the major limitation for wide use in industrial applications.

In this paper, we present a heterodyne interferometer using photorefractive cubic crystal  $\text{Bi}_{12}\text{SiO}_{20}$  (BSO) in a two-wave mixing configuration. The combination of heterodyne detection with the photorefractive process results in a well proven noise insensitive technique with a large étendue (ability to work on rough surfaces). In our case, by using a low gain and fast time response PRC such as BSO, the low frequency (less than kHz) and large amplitude noise that creates decorrelation and large phase shift of the speckle signal can be compensated. The heterodyne technique allows automatic absolute calibration of the displacement.

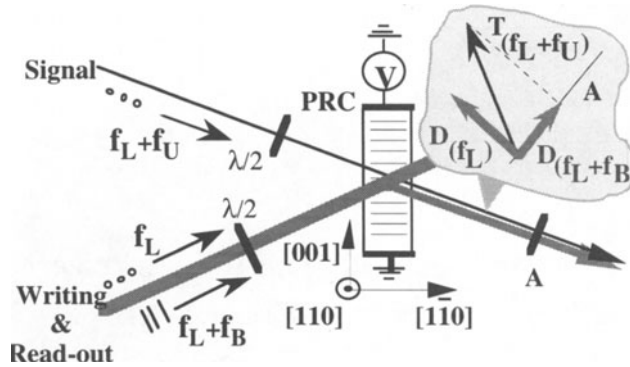


Figure 1. Wave mixing configuration. T:transmitted; D:diffracted; A:analyzer.

## INTERFEROMETER DESIGN

The schematic for wave mixing in the photorefractive crystal is shown in Fig. 1. The signal beam which is scattered by the rough surface of the specimen under study and a reference (writing) beam interfere inside the photorefractive crystal. Both beams are polarized along the same direction. For heterodyne detection, a third beam (the reading beam) with its polarization  $90^\circ$  rotated and its frequency shifted by  $f_B$  is aligned with the writing beam. The writing and reading beams are thus collinear but with cross-polarizations and two different frequencies, respectively  $f_L$  and  $f_L + f_B$ , where  $f_L$  is the laser beam frequency. Only the grating due to the homodyne interference between the writing and the signal beams is created in the photorefractive crystal. Here the grating vector is along the [001] crystal axis. Using this geometry, the diffracted beam has its polarization axis aligned with the polarization axis of the transmitted beam. Following the standard theory of the photorefractive effect, the intensity detected after the analyzer can be written as [3]:

$$I(t) = |\gamma_{Ta}|^2 I_S + |\gamma_{Da}|^2 I_P + |\gamma_{D'a}|^2 I_{P'} + 2|\gamma_{Ta}||\gamma_{Da}|\sqrt{I_P I_S} \cos(\varphi(t) + \varphi_T - \varphi_D) + 2|\gamma_{Ta}||\gamma_{D'a}|\sqrt{I_{P'} I_S} \cos(2\pi f_B + \varphi(t) + \varphi_T - \varphi_{D'}) + 2|\gamma_{Da}||\gamma_{D'a}|\sqrt{I_{P'} I_P} \cos(2\pi f_B + \varphi_D - \varphi_{D'}) \quad (1)$$

where  $I_S$  and  $I_P$  are respectively the intensities of the signal and writing pump beams,  $I_{P'}$  is the intensity of the read-out beam.  $\gamma_T$  and  $\gamma_D$  are the amplitude of the transmission coefficient for the signal beam and the diffraction coefficient for the writing pump beam, respectively.  $\gamma_{D'}$  is the amplitude of the diffraction coefficient for the read-out pump beam. The index  $a$  indicates the projection along the direction of the analyzer,  $\varphi_T$ ,  $\varphi_D$ , and  $\varphi_{D'}$  are the phase terms of  $\gamma_T$ ,  $\gamma_D$ , and  $\gamma_{D'}$ , respectively.  $\varphi(t)$  is the small induced phase shift caused by the ultrasonic signal. In the case of harmonic ultrasonic signal and normal incidence of the signal beam on the specimen, the induced phase shift is  $\varphi(t) = 2k_0 U_N(t)$ , with  $U_N(t) = \delta \sin(2\pi f_U t)$  where  $\delta$  is the displacement amplitude and  $f_U$  is the frequency of the ultrasonic signal.

From eq. 1 we can see that a homodyne detection coexists with the heterodyne detection. By choosing  $f_B$  large enough, the homodyne detection can be separated from the heterodyne detection. One advantage of using a heterodyne detection is the possibility of automatic absolute calibration. For doing that the signals at frequencies  $f_B$  and  $f_B \pm f_U$  are compared. Because the last term of eq. 1 is at the frequency of the carrier  $f_B$ , it will perturb the calibration. Thus, in order to optimize the heterodyne detection of  $\varphi(t)$  we must have:

$|\gamma_{Da}| = 0$ . In this case eq. 1 reduces to the classical equation of heterodyne detection using a Mach-Zehnder configuration.

In a first step, without the analyzer, the polarization angles are adjusted using a half-wave plate in order to maximize the heterodyne component  $\gamma_D$ . The direction of the analyzer is adjusted to block the homodyne diffracted signal,  $|\gamma_{Da}| = 0$ . Then, by adjusting the polarization of the signal beam, we allow a component of the signal beam to be transmitted by the analyzer such as  $|\gamma_{Ta}|^2 I_S = |\gamma_{D'a}|^2 I_{P'}$ , corresponding to maximum modulation depth of the interference heterodyne signal.

Because of the simultaneous presence of induced linear birefringence and natural optical activity, the polarizations after propagation through the crystal become elliptical. There is a small component of the diffracted beam at frequency  $f_L$  that is transmitted through the analyzer, reducing the modulation depth of the carrier signal. The ellipticity of the polarization being small [4], this diffracted homodyne beam is of small amplitude. It must also be noted that now a component of the signal beam will interfere with the read-out beam. Fortunately, because of the frequency difference between both beams, the non-stationary fringe pattern will not be recorded in the PRC.

## EXPERIMENTAL RESULTS

The experimental set-up is described in Fig. 2. We use a 600mW Argon laser emitting at 514nm. The frequency shift  $f_B$  introduced by the Bragg cell is 40MHz. An ac sinusoidal electric field of 7.8kV/cm is applied along the <001> crystallographic axis of a 5x10x10mm<sup>3</sup> BSO crystal.

Figure 3 shows the instantaneous signal recorded on a rough aluminum surface. The ultrasonic signal is generated using a surface wave piezoelectric transducer of 5MHz central frequency. Generation and detection are on the same side of the aluminum specimen. The total intensity onto the crystal is 1.6W/cm<sup>2</sup> and the intensity received onto the photodiode is 0.56 mW. The heterodyne signal from the photodiode is demodulated to provide an electric signal directly related to the temporal phase variation of the ultrasonic signal [5].

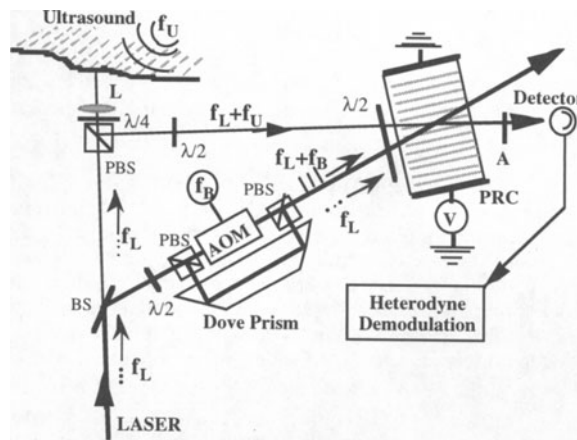


Figure 2. Basic setup for heterodyne detection of ultrasound by wave mixing in PRC. BS: beam splitter; AOM: acousto-optic modulator; PBS: polarizing beam splitter; A: analyzer; and L: lens.

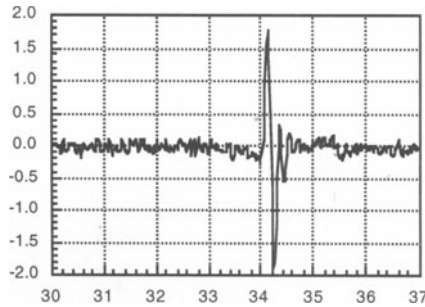


Figure 3. Instantaneous ultrasonic signal detected on a rough aluminum specimen.

Assuming that the sensitivity is limited by the shot noise level of the photodiode and the dark current is negligible, the SNR for the heterodyne interferometer in the case of double side-band detection can be expressed as [6]:  $SNR = k_0 \delta M \sqrt{\eta I_0 / (4 h \nu \Delta f)}$ , where  $I_0$  is the dc component of the incident light power,  $M$  is the modulation depth of the carrier signal,  $\eta$  is the detector's quantum efficiency,  $h\nu$  is the photon energy,  $\Delta f$  is the detection electronics bandwidth. In our experiment, the modulation depth  $M$  of the heterodyne signal was 40%. The electronic detection bandwidth used is 15 MHz and the rms noise level measured from the instantaneous signal is 0.066 nm, corresponding to a sensitivity [6] of  $0.42 \times 10^{-5} \text{ nm} \sqrt{W/Hz}$ . In our experiment, using  $\eta=0.4$  and  $M=40\%$ , we find the theoretical shot noise limited sensitivity to be  $0.40 \times 10^{-6} \text{ nm} \sqrt{W/Hz}$  which is close to the value experimentally measured.

Figure 4 shows an example of application to laser-based ultrasonic. In this experiment, the generation of surface wave is done using a Nd-YAG laser of 15 mJ. The laser beam is focused to a line, resulting to the propagation direction of the acoustic surface wave to be perpendicular to the line. The distance between emitter and receiver is 70 mm and the receiver is at 30 mm from the edge of the plate. The plate thickness is 25 mm. We can clearly see the direct surface wave R and the surface wave reflected by the edge RR. The bulk waves reflected by the back face of the plate are also visible. P1 and P3 are the compressional wave that undergo one and three reflections, respectively. S1 is the shear wave that undergoes one reflection.

An other example of application to NDE is shown in figure 5. In this experiment, laser-based ultrasonic is investigated on composite material. A graphite epoxy composite material made of 100 unidirectional layers is used. The surface finish of the composite material is of black color. The laser generation is identical to the previous experience. The detection is achieved without any surface preparation of the composite material. Due to the poor reflection of the composite surface, the object intensity decreases by a factor 16 compared to the previous experience with detection on rough aluminum. This decrease of signal intensity leads to an increase of the noise level. For this experiment, we find a sensitivity of  $S=2.1 \times 10^{-5} \text{ nm} \sqrt{W/Hz}$ . Figure 5 shows the recorded wave for propagation along the direction of the fibers as well as for propagation perpendicular to the fiber direction. As expected, due to the higher velocity in the graphite fibers, the surface wave propagating along the direction of the fiber is faster than the surface wave propagating perpendicular to the direction of the fibers.

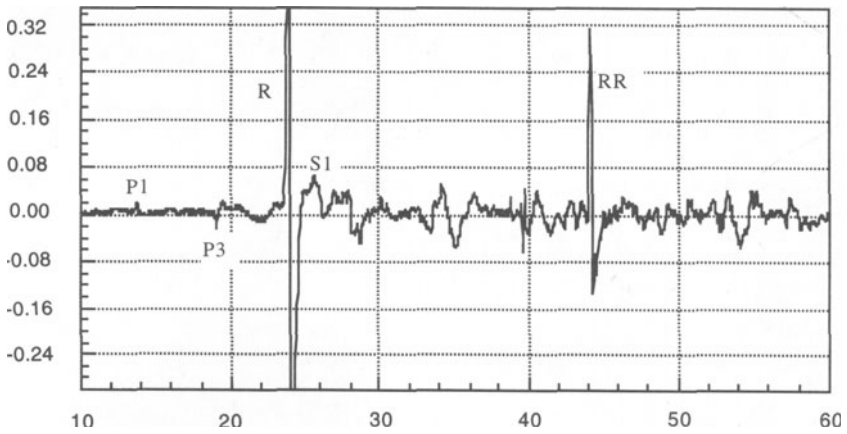


Figure 4. Laser-generated ultrasonic signal detected on a rough aluminum plate.

## CONCLUSIONS

We have described a heterodyne interferometer using beam coupling in a photorefractive cubic crystal. Because the photorefractive grating generates a matched wavefront for interference, this interferometer is characterized by a large étendue. The main advantage in using cubic crystals is their relative fast response compared to ferroelectric crystals which allows them to work in a noisy environment with reasonable laser power. Further improvement of the time response can be obtained by using semi-conductor photorefractive crystals. The sensitivity is essentially independent of the speckle nature of the signal beam reflected or scattered by the inspected material. This interferometer is therefore useful for applications where noise and stability are problematic when a specimen with a rough surface is tested.

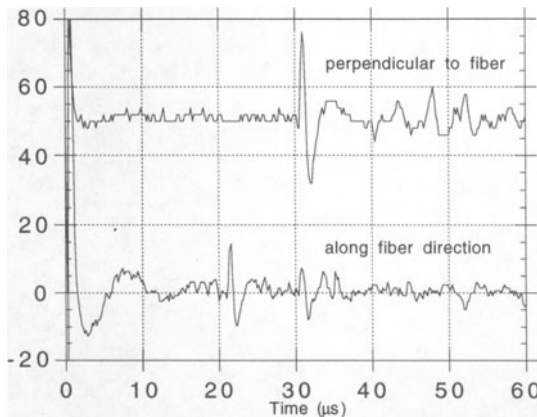


Figure 5: Ultrasonic signal detected on a graphite-epoxy composite specimen.

## REFERENCES

1. J. P. Monchalin, "Optical detection of ultrasound", *IEEE Trans. Ultrason. Ferroelectr. Freq. Control*, vol 33, pp. 485-499, 1986.
2. R. K. Ing, J. P. Monchalin, "Broadband optical detection of ultrasound by two-wave mixing in a photorefractive crystal", *Appl. Phys. Lett.* vol. 59, pp. 3233-3235, 1991.
3. R.K. Ing, D. Royer, B.F. Pouet, Sridhar Krishnaswamy, "Ultrasound detection on rough surfaces using heterodyne photorefractive interferometer: applications to NDE," *1996 IEEE Ultrasonics Symposium*, pp. 681-684, San Antonio, 1996.
4. A. Marrakchi, R. V. Johnson, A. R. Tanguay, "Polarization properties of enhanced self-diffraction in sillenite crystals", *IEEE J. Quant. Elec.* vol. QE-23, pp. 2142-2151, 1987.
5. D. Royer and E. Dieulesaint, *Rev. Phys. Appl.* vol. 24, p. 833, 1989.
6. J. W. Wagner and J. B. Spicer, "Theoretical noise-limited sensitivity of classical interferometry", *J. Opt. Soc. Am. B*, vol. 4, pp. 1316-1326, 1987.